

A Study on Physical, Morphological and Antibacterial Properties of Bio Polymers Reinforced Polyvinyl Acetate Foams

Nadir Yildirim^a, Ertan Ozen^b, Mehmet Emin Ergun^{c*} , Berk Dalkilic^d

^aHamad Bin Khalifa University, Doha, Qatar.

^bMuğla Sıtkı Koçman University, Faculty of Technology, Department of Woodworking Industrial Engineering, Muğla, Turkey.

^cAlaaddin Keykubat University, Akseki Vocational School, Department of Forestry, Antalya, Turkey.

^dSinop University, Ayancık Vocational School, Department of Design, Sinop, Turkey.

Received: November 14, 2021; Revised: June 12, 2022; Accepted: July 19, 2022

In this study, foaming-agent free novel polyvinyl acetate (PVAc) foams reinforced with bio polymers were manufactured through freeze-drying technique. The physical, morphological and antibacterial properties of foams which were reinforced with different ratio of zinc borate and water-soluble chitosan were investigated according to relevant standards. The PVAc foams showed low densities (0.12 g/cm³ – 0.21 g/cm³) and high porosity rates (87.50% - 79.05%). The results showed that although the foams have no antibacterial character against *Escherichia Coli*, they have antibacterial character against *Staphylococcus Aureus* bacteria. This study mainly focusses on physical and morphological properties of the foams. However, researchers also performed accelerated weathering tests to determine its usability in different industries. The effects of accelerated weathering on the surface of foams were investigated by measuring surface color. The highest color difference was determined 8.09. This foam can be used as a low-density packaging material and/or medical box with its promising physical and morphological properties with hazardous-chemical free structure.

Keywords: Antibacterial effect, bio polymers, freeze-drying, polyvinyl acetate (PVAc) foam.

1. Introduction

Foams consist of solid polymeric matrix and gas phase which are generally obtained with a foaming agents, such as pentane, and hydrochlorofluorocarbon¹. However, these foaming agents are highly flammable and harmful to both human health and the environment². These are used for creation of voids in the foam to reduce the density and increase the thermal insulation properties, also produces decrease in the amount of raw material needs to be used to manufacture the foams^{3,4}. Conventional raw materials such as polystyrene, polyurethane, polyvinyl chloride, and polyolefin are extensively utilized as the matrix of foams and they are commonly used in insulation, cushioning, packaging of valuable goods and food packaging fields. But due to the inadequate recyclability and decomposability of these materials, most of the foams are wasted at the end of their product life. This creates increase in pollution^{5,6}.

Although PVAc is a synthetic polymer, it is consumed by *Penicillium* and *Aspergillus* fungi species in laboratory conditions⁷. Based on its versatility of structure and related properties⁸, PVAc usually utilizes as an adhesive in wood industry. Recently, it has shown potential for use in development of composite materials⁹, films¹⁰ and foams¹¹. Biopolymer additives, such as calcium carbonate¹², nanocellulose¹³, and sisal cellulose¹⁴, were incorporated into the PVAc matrix to prepare sustainable products with improved properties. The addition of reinforcement of higher strength than the

matrix polymer improves the mechanical properties of plastic resins. Carbon nanotubes and carbon fibers are studied to improve the mechanical performance of reinforced polymers, and they are commonly used for polymer reinforcement¹⁵⁻¹⁸. However, there are some problems related to the use of synthetic fiber-reinforced composites. When it comes to synthetic reinforcements, waste disposal and recycling are important issues all around the world. Disposal of waste is significantly excluded on a global scale due to increasing environmental awareness. Therefore, researchers were focused on environmentally compatible reinforcement materials in recent years¹⁹⁻²¹.

Cellulose is a natural biopolymer that is renewable, biodegradable and non-toxic. It is the most abundant natural biopolymer in the world. Cellulose occupies 40% – 50% of the earth's total biomass reserves²². Cellulosic fibers have advantageous compared to synthetic fibers. The natural fibers bend rather than break (fail) during processing and manufacturing²³. In addition, cellulose has a flattened oval cross-section, which enhances stress transfer by presenting a higher aspect ratio²⁴.

The most challenging issue with use of cellulose-based materials for packaging purposes is their vulnerability to microbial growth^{25,26}. Polyhexamethylene guanidine hydrochloride²⁷, copper oxide²⁸, zinc oxide²⁹ and silver³⁰ are used to acquired antibacterial properties to the foam material and they have a great protection against gram positive and gram negative bacterias. The majority of commercial

*e-mail: mehmet.ergun@alanya.edu.tr

antibacterial products are based on a leaching technique, in which biocides are introduced into the material and leached into the environment to destroy microorganisms. Silver particles are widely utilized for this aim, despite the fact that silver ions are venomous to mammalian cells and can result in silver-resistant bacteria^{31–33}. Therefore, the focus has been on alternative antimicrobial polymers that do not harm mammals. Chitosan, which is produced by deacetylation of chitin, is the second most abundant polymer in nature, has widespread use in many areas due to its antibacterial and antifungal properties³⁴. This is frequently owing to intense interactions between the positively charged groups of the polymer and the negative charges on the bacterial and fungal cell walls^{35,36}. Cell walls are negatively charged on the surface, and cationic polymers bind to anionic components on the cell walls of microorganisms, changing the permeability of the cell wall and leading to cell death^{34,37}.

Many foam manufacturing methods has been studied both commercially and scientifically. The well-known methods can be named specifically, extrusion³⁸, injection molding³⁹ and batch process⁴⁰, melting the raw materials under high temperature and providing the formation of highly porous final product (foam) using foaming agents⁴¹. Although the production time is very short with these techniques, they do not allow pre-surface modification. Because the chemicals used during surface modification degrade at high temperatures during foam production and have a negative effect on the materials⁴². On the other hand, many studies have been carried out on the freeze-drying technique that enables the production of more qualified products and allowing surface modification^{43–45}.

The freeze-drying procedure is divided into three stages: freezing, primary drying, and secondary drying⁴⁶. During the freezing process, the water molecules create ice crystals in the first part. The drying process then begins under particular pressure and temperature settings. As ice crystals sublimate during the drying step, the final pore shape is formed. As a result, the foam structure is directly relevant to the dispersion and size of the frozen system⁴⁷.

Biopolymer-based foams for different purposes were produced with the freeze-drying technique. For instance; the highly porous, low density, and cross-linked natural cellulose foams which modified with silane based hydrophobic chemical from rice straw was produced. These cellulose foams can be utilized as a worthwhile sorbent for adsorption of oil and organic solvents⁴⁸. Another study, polyvinyl alcohol reinforced cellulose-based foams were produced from waste fibers

which have good thermal property. Density and porosity value of foams were 0.019–0.046 g/cm³ and more than 96%, respectively. These foams exhibited good heat insulation with low thermal conductivity (0.039–0.043 W/m K) due to the porous structure inside⁴⁹. The produced cellulose foams have a low density (0.0554 g/cm³), good thermal stability, and a high porosity (89.32%). Furthermore, directed cellulose foams exhibit good mechanical properties, with a compressive stress of 0.35 MPa at 70% strain. The cellulose foams that have been treated with directed freezing have promising applications in the field of sound absorption⁵⁰. Alumina reinforced polyvinyl alcohol/chitosan-based foam produced and they have the smoke-suppressant, high-strength and fire-retardant. It stated that foams used for potential alternatives to traditional flame-retardant foams. It was stated that the produced foams can be used as potential alternatives to conventional flame retardant foams⁵¹.

The novel idea presented in this study is to design and development of PVAc foams with bleached kraft pulp, water-soluble chitosan and zinc borate and investigating their physical and morphological properties.

2. Materials and Methods

2.1. Material

In this work, the polyvinyl acetate (Figure 1a) (PVAc: Mad Wolf brand, made in Akpınar Building Materials Industry and Trade Inc./Istanbul) was bought from a local supplier. The solid content of PVAc was 42.8%. The density of PVAc was 1.2 g/cm³. The brightness value of bleached kraft pulp was 90% (ISO 2470), and the degree of polymerization was 933, was supplied from EUROPAP (İzmir, Turkey). The density of bleached kraft pulp (Figure 1b) which was produced from Eastern Spruce was 0,55 gr/cm³, and the pulp was bleached elementary chlorine free (ECF). Zinc borate (Figure 1c) (Zn₃BO₆) (Kimetsan Chemistry) had a purity degree of 85.27% and the density of zinc borate was 2.6 g/cm³. Chitosans were purchased from Sigma-Aldrich in low (50000-190000 Da), medium (200000-300000 Da) and high molecular (310000-375000 Da) weights. Glycidyltrimethylammonium chloride (GTMAC) (Sigma-Aldrich) was used in the synthesis of water-soluble chitosan (Figure 1d).

2.2. Modification of chitosan

Chitosan is soluble in acidic condition. Acidic condition was led to degrade polyvinyl acetate. Therefore, in this study was needed to synthesize water-soluble chitosan. Initially,



Figure 1. Materials used in foam production a. PVAc, b. Bleached kraft pulp, c. Zinc borate, d. Water-soluble chitosan.

chitosan (30.00 g) was dispersed in 300 ml water. After that, the glycidylthymethylammonium chloride (GTMAC) (112.90 g) was added, and the mixture was stirred at 80 °C for 8 h. The reaction products were filtered, concentrated, precipitated in acetone, and dried at 60 °C for overnight to obtain the water-soluble chitosan.

2.3. Foam preparation

This study was conducted in two sections. The first section, has investigated the effects of zinc borate in different ratios. In the second section, the optimum zinc borate ratio was kept constant, and the effects of molecular weights and ratios of water-soluble chitosan were investigated on foams. Ingredient of the foam were given in Table 1. Mixtures were blended for 15 minutes at 2000 rpm after each reinforcement addition.

Table 1. Ingredient of the PVAc foam reinforced with the different bio polymers.

Codes	Polyvinyl Acetate (g/L)	Bleached Kraft Pulp (g/L)	Zinc Borate (g/L)	Water-Soluble Chitosan (g/L)
Z-1	100	80	20	0
Z-2	100	80	60	0
Z-3	100	80	100	0
C-1	100	80	60	30 ^x
C-2	100	80	60	50 ^x
C-3	1100	80	60	70 ^x
C-4	100	80	60	30 ^y
C-5	100	80	60	50 ^y
C-6	100	80	60	70 ^y
C-7	100	80	60	30 ^z
C-8	100	80	60	50 ^z
C-9	100	80	60	70 ^z

^x: Low molecular weight water soluble chitosan, ^y: Medium molecular weight water soluble chitosan, ^z: High molecular weight water soluble chitosan.

All samples were poured into the mold, and they were frozen at -25 °C for 24 hours. The frozen samples were freeze-dried in a lyophilizer (ModulyoD, Termo Savant) at a condenser temperature of -50 °C under 0.40 mBar pressures for 48 hours to produce the foams. The preparation method of PVAc foams was shown in Figure 2.

2.4. Characterization

2.4.1. Determination of molecular weight

A molecular weight measurement of chitosan and water-soluble chitosan were analyzed with a Ubbelohde viscometer. Viscosity values of chitosan solutions were prepared in a mixture of 0.25 M acetic acid and 0.50 sodium acetate solvent to concentrations of 0.10 to 0.50 g/dl, depending on the sample⁵². The reduced viscosity (η) values were found from the equations of the curves of the graphs drawn with the determined η_{sp}/c values. Then, the molecular weights of chitosan were determined according to the following Mark-Houwink Equation 1.

$$[\eta] = K \cdot M^{\alpha} \quad (1)$$

where $[\eta]$ is the intrinsic viscosity and M is molecular weight. The constants, α and K , are 0.79 and $1.57 \cdot 10^{-4}$ dl/g, respectively⁵³.

2.4.2. FTIR spectrum

FTIR measurements were used to determine changes in the chemical structure of water-soluble chitosan. For this purpose, FTIR (Thermo Fisher Scientific brand Nicolet™ iS10) device was used and measurements were made in the spectra range of 600-4000 cm^{-1} . The data obtained as a result of the measurement process were visualized with OMNIC™ Spectra Software.

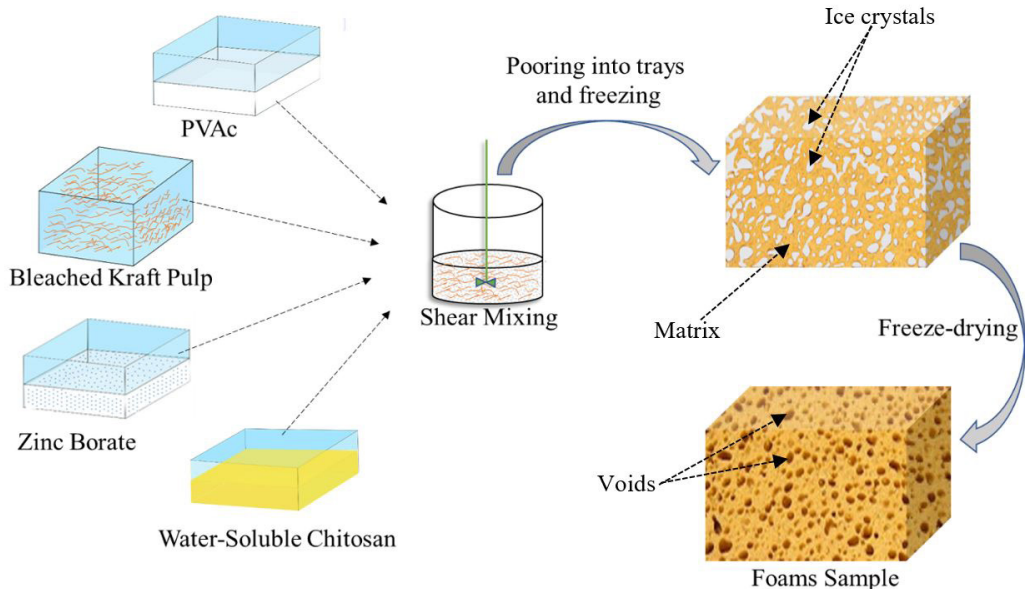


Figure 2. Manufacturing process of PVAc foams reinforced with bio polymers.

2.4.3. Density and porosity determination

Produced PVAc foams (Figure 3) were held in laboratory conditions for 24 hours for conditioning. The seven (7) samples with 10 mm x 50 mm x 50 mm dimensions from each group were measured according to ASTM C303 (2010) standards.

The porosities of the developed foams were determined by the formulas given below (2).

$$P_f = 100 \times \left(1 - \frac{d_{\text{bulk}}}{d_{\text{particle}}}\right) \quad (2)$$

P_f = porosity (%)

d_{bulk} = density of foam (g/cm³)

d_{particle} = density of particle (g/cm³)

2.4.4. Antibacterial activity test

The disc-diffusion method was used to determine the antibacterial activity. As test organisms, 24-hour cultures of *Escherichia Coli* and *Staphylococcus Aureus* bacteria were used. After inoculation of 100 µl with the help of a drigalski spatula, 0.5 McFarland dilutions were prepared from liquid cultures of test microorganisms in petri dishes containing Iso-Sensitest agar (Oxoid CM0471), and the petri dishes were incubated for one hour. Then, specimens prepared with different materials and cut into 10 mm diameter discs were placed in petri dishes. After this process, the petri dishes were examined after 48 hours of incubation at 30°C and the zone of inhibition (ZOI) formed was measured.

2.4.5. Morphological structure

The morphologies of the foams were examined using a JSM-7600F brand scanning electron microscope (SEM). The surfaces of the foams were coated to increase conductivity with gold. During the examination of the microstructure images, the operating voltage of the microscope was chosen as 15 kV.

2.4.6. Accelerated weathering test and color measurement

The accelerated weathering test was carried out in a QUV weathering device (Q - Lab, USA) outfitted with eight UVA 340 lamps in accordance with the ASTM G154 (2006) standard. For a total of 50 hours, foams were exposed to cycles of 8 hours UV-light irradiation followed by 4 hours condensation in the accelerated weathering test device. At the maximum intensity of 340 nm wavelengths, the average

irradiance was 0.89 W/m² (max = 340 nm). The temperatures during the light irradiation and condensation periods were 60 °C and 50 °C, respectively.

The CIEL*a*b* method was used to calculate the color parameters L*, a*, and b*. The lightness is represented by the L* axis, while the chromaticity coordinates are represented by a* and b*. The parameters +a* and -a* represent red and green, respectively. The +b* parameter represents yellow, while the -b* parameter represents blue. L* can range from 100 (white) to 0 (black). The colorimeter (X-Rite SP Series Spectrophotometer) was used to measure the colors of the specimens before and after accelerated weathering. The color differences of foams (ΔE) were determined according to ASTM D1536–58 T (1964).

2.4.7. Statistical analysis

All results were compared using one-way means/ANOVA to check for significant differences (alpha=0.01). The Tukey-Kramer Honest Significant Differences (HSD) test (alpha=0.05) was used to examine whether there were significant differences between the groups.

3. Results and Discussions

3.1. Determination of molecular weight

In this study, water-soluble chitosan was used to prevent the degradation of the PVAc matrix in acidic conditions. As a result of the viscosity measurements, the intrinsic viscosities ($[\eta]$), molecular weights and densities of chitosan before and after synthesis were given in Table 2.

Molecular weights of water-soluble chitosan which were synthesized via glycidyltrimethylammonium chloride (GTMAC) were decreased because intermolecular bonds of chitosan were broken in the alkaline condition⁵⁴.

3.2. FTIR spectrums of chitosan and water-soluble chitosan

The GTMAC was used in the production of water-soluble chitosan. The general chemical structures of chitosan synthesized with GTMAC, and the determination of the changes in the chemical structures after synthesis have been demonstrated by FTIR diagrams as given in Figure 4.

The NH₂ group, which was the characteristic peak of water-soluble chitosan, was observed at approximately 1646 cm⁻¹. In addition, a new peak was formed at 1479 cm⁻¹. This weak peak was observed due to the binding of ammonium

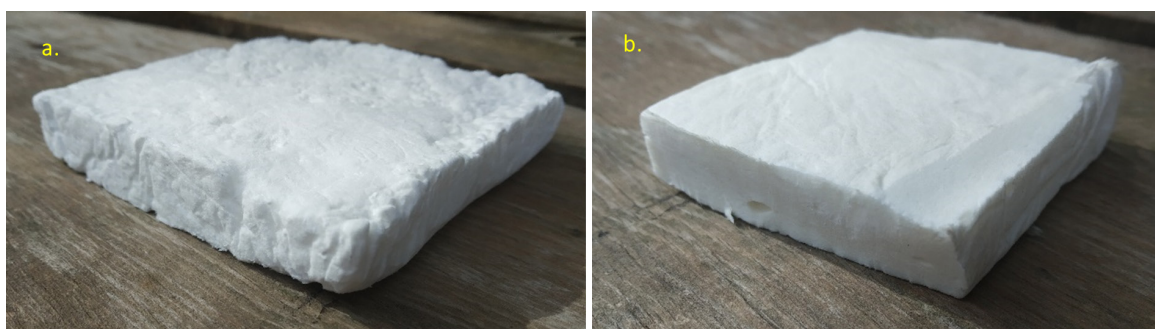


Figure 3. Produced PVAc foams (a. Z-2, b. C-6).

Table 2. Intrinsic viscosity, molecular weights and density of chitosans and water-soluble chitosans.

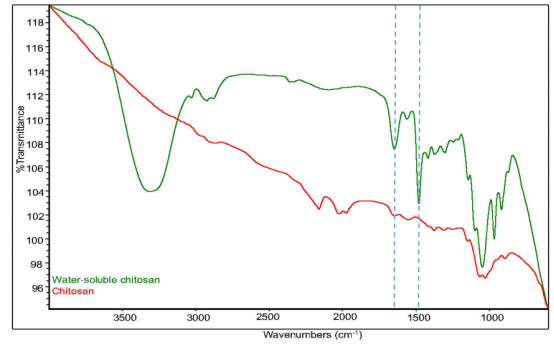
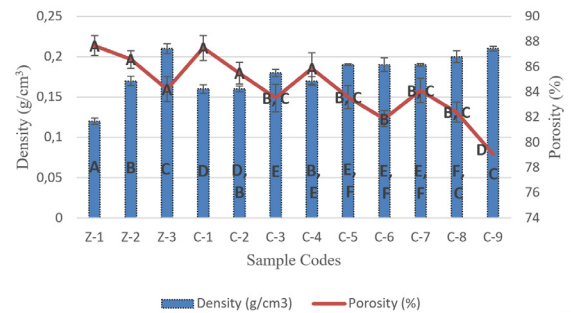
Chitosan Type	Intrinsic Viscosity [η]	Molecular Weight (Da)	Density (g/cm^3)
High Molecular Weight Chitosan	3.85	333959	0.34
Medium Molecular Weight Chitosan	2.61	208039	0.26
Low Molecular Weight Chitosan	1.96	145013	0.18
Water Soluble High Molecular Weight Chitosan	1.92	141294	0.24
Water Soluble Medium Molecular Weight Chitosan	1.26	83106	0.16
Water Soluble Low Molecular Weight Chitosan	0.67	37499	0.12

groups to methyl groups. On other hand, the presence of a quaternary amine group, which allowed chitosan to dissolve in water after modification with this peak, was determined⁵⁵.

3.3. Density and porosity determination

The variation on the porosity and density values depending on the reinforcements were given in Figure 5. The test results showed that the concentration ratio of zinc borate and water-soluble chitosan changed the density and the porosity as expected.

Density values depending on concentration ranged from $0.12 \text{ g}/\text{cm}^3$ to $0.21 \text{ g}/\text{cm}^3$. The highest value was obtained from C-9 which high molecular weight water-soluble chitosan at $70 \text{ g}/\text{L}$ concentration. Z-1 gave the lowest density value with $0.12 \text{ g}/\text{cm}^3$ and C-9 gave the highest density value with $0.21 \text{ g}/\text{cm}^3$. Due to fibers clump, attractive forces (intermolecular forces and capillary) and particles and adhere together during solvent removal. This phenomenon led to occur more dense foams. Besides, although particle dimensions can be influenced by the source, fiber-based foams can benefit from the natural morphology of the cellulose source⁵⁶. Selecting naturally lightweight fibers (highly porous and/or hollow lumen), such as bleached kraft pulp which was used in our study ($0.55 \text{ g}/\text{cm}^3$), is an obvious way to reduce density. Other low-density fibers are found, for example, in bamboo⁵⁷ ($0.26\text{--}1.21 \text{ g}/\text{cm}^3$), flax⁵⁸ ($0.34\text{--}0.74 \text{ g}/\text{cm}^3$), jute⁵⁹ ($0.41\text{--}0.78 \text{ g}/\text{cm}^3$) and sugarcane bagasse⁶⁰ ($0.10\text{--}0.49 \text{ g}/\text{cm}^3$). On the other hand, shrinkage occurs when materials were freeze-dried, and it was shown that shrinkage can reduce the volume of foams by up to 30%⁶¹. The porosity values in Figure 5 and voids in Figure 6 provided qualitative information about how the pore ratio diminishing with increasing amount of water-soluble chitosan and zinc borate in suspensions after freeze-drying, occurring a decrease in porosity. Porosity values depending on concentration found between 87.50% to 79.05%. C-9 were given the lowest porosity values with 79.05%. The highest porosity value was obtained from Z-1 with 87.50%. The pore sizes and ratio decrease with an increase in the amount of water-soluble chitosan in the samples. The ice templating theory of suspensions can articulate that case⁶¹. According to this theory, the higher cellulose and water-soluble chitosan

**Figure 4.** FTIR spectra for chitosan and water soluble chitosan.**Figure 5.** Density and porosity results of foams (A, B, C, D, E, and F letters indicate the significant differences between the groups).

content in the gels prevents broader interconnected ice crystal formation during the ice templating process, resulting in smaller pores ratio and size distribution in the samples after freeze-drying. Also, partly low amount of cellulose and water-soluble chitosan during the ice templating step, because of the lower resistance to ice crystal formation, higher porosity gels with varied pore size and ratio distributions were produced⁶². In addition, during the freezing process of water, ice crystals nucleate, develop, and concentrate cellulose in the interstitial spaces between crystals, lead to the formation of aggregated foam cell walls⁶³. Additional aggregation is very likely to occur during the sublimation phase. As a result, the porosity of the foams is diminishing⁶⁴.

Cellulose-based foams were produced with different drying techniques before. For example, freeze-drying⁶⁵⁻⁶⁷ or ambient drying, supercritical drying⁶⁸. The density of the material produced via supercritical drying (nanopaper) is $0.64 \text{ g}/\text{cm}^3$ and that of foams made from varibale forms of ambient drying⁶⁹ varies between $0.033 \text{ g}/\text{cm}^3$ and $0.066 \text{ g}/\text{cm}^3$. The foam produced in this study, with a density of 0.12 to $0.21 \text{ g}/\text{cm}^3$ is definitely equivalent to these materials, as well as expanded polystyrene foam⁷⁰ (EPS) with a density ranging from 0.02 and $0.64 \text{ g}/\text{cm}^3$. In our study, the porosity of the foam, which varies from, 87.68 to 79.05% , is comparable with other cellulose based foams⁷¹.

In this study, it was observed solid content of foams considerably affected the final density and porosity. In previous studies, the density and porosity of foams produced from chitosan and silica were found between $0.07 \text{ g}/\text{cm}^3$ to

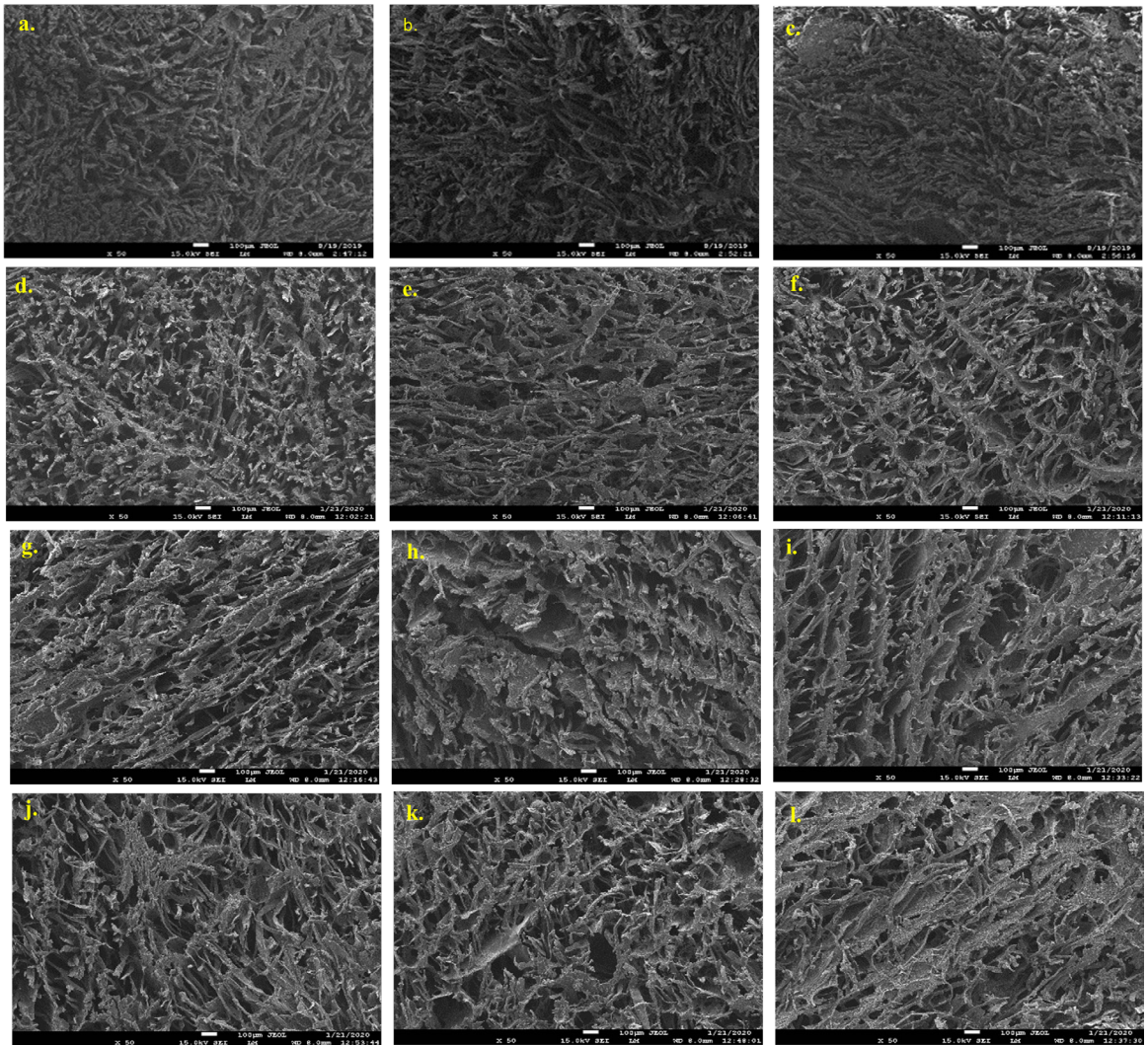


Figure 6. The SEM images of PVAc foam reinforced with different rate of zinc borate (a. Z-1, b. Z-2, c. Z-3) and different rate and molecular weight of water-soluble chitosan (d. C-1, e. C-2, f. C-3, g. C-4, h. C-5, i. C-6, j. C-7, k. C-8, l. C-9) at x50 magnifications.

0.25 g/cm³ and 81.60% to 97.50%, respectively⁷². The density of the samples produced with wood fiber, cellulose nanofiber and cationic polyacrylamide varied between 0.01 g/cm³ and 0.06 g/cm³, and the porosity rate was found over 90%⁶⁹. The porosity values of the composite material produced from bacterial cellulose changed between 33.70% to 57.40%⁷³. The density of foams produced from tapioca starch bleached kraft pulp and chitosan varied between 0.12 g/cm³ and 0.15 g/cm³. In addition, it was determined that the density of the foams increased as chitosan and fiber content increased⁷⁴. Pakornpadungsit et. al. (2020) stated that the porosity value of the materials produced for porous tissue scaffolds from deoxyribonucleic acid sodium salt and chitosan varies between 49% and 62%⁷⁵. Chitosan-based aerogels reinforced with microcrystalline cellulose and their density and porosity values ranged 0.03 g/cm³ to 0.11 g/cm³ and 94.73% to 62.30%, respectively¹⁹. As a result, the density and porosity values of the PVAc foams in this study were found to be compatible with the literature.

3.4. Morphological structure

The microstructures of the foams were investigated at x50 magnification using Scanning Electron Microscope as given in Figure 6. The hierarchical irregular pore formations with variable diameters were seen.

The amount of PVAc and bleached kraft pulp were kept constant and the effect of the zinc borate (a, b, c) and different molecular weights of water-soluble chitosan reinforcement (d to l) on the foams were investigated in Figure 6. The increase in zinc borate and water-soluble chitosan amount decreased the inter-pore gap, and the more stringent structures were observed. The freeze-dried foams obviously demonstrate a network interconnected porous structure. Foams exhibits an irregular porous layered structure (Figure 6a, b, c) which is the path left by the ice crystals comprise of same directions after freeze-drying. The structures of the foams change due to the amount of zinc borate and water-soluble chitosan. Water soluble chitosan molecules are taken shape into large blocks after the addition, restricting the mass mobility and

affecting their rearrangement at the borders between the growing ice crystals⁷⁶. However, increasing the amount of water-soluble chitosan leads in an increase in solution viscosity, which retarding the ice crystal growth when frozen. When the concentration of water-soluble chitosan reaches 70 g/L, the lamellar structure is replaced by a tight architecture (Figure 6f, i, l) due to an increase in solution viscosity and a decrease in mass mobility of precursor solutions⁷⁷. Because of the strong hydrogen bonding, when zinc borate is introduced to the precursor solution, the zinc borate is encapsulated by water-soluble chitosan molecules^{78,79}. Moreover, some water-soluble struts can be found bridging the gaps between zinc borate particle (Figure 6h, k). It is known that matrices containing hydroxyl groups can form hydrogen bonds with inorganic particles⁸⁰.

The amount of bleached kraft pulp was kept constant in this study because our previous study was investigated to effect of bleached kraft pulp amount¹¹. The bleached kraft pulp led to decreased the inter-pore gap. Although the morphological structure of nano-fibril cellulose and starch foam material had uniform pore shapes^{47,81}, morphological structure of PVAc foams was shown to be tight structure and irregular pore shape. The individual particle size of the bleached kraft pulp was in the macro dimension. This macro dimension disturbed inter-pore gaps and structure. Similar tight and irregular structure were procured with bleached kraft pulp-based foams^{34,69}.

Zinc borate particles were aggregated on bleached kraft pulp. When the amount of reinforcement ingredients increased, the density increased, and a tighter structure was formed. In addition, water-soluble chitosan, like PVAc, was found to contribute to the cell wall formation of foams. Also, no foaming agent was used in the foam process. The separation of solvent and solute occur due to most solutes cannot fit within the formed ice crystal structure. So, the final pore morphology was given rise to as ice crystals were sublimated during the drying step⁸². MatLab software was used to investigate pore size determination. There was a wide range of pore sizes determined. Pore diameters ranged from a few micrometers to several millimeters. The primary cause of this variation is assumed to be related to the manufacturing process, in which the sublimation process could not be regulated uniformly.

In previous studies, the foam - produced with the freeze-drying technique was examined and the morphological structure of foams had a honeycomb appearance^{47,81,83}. But in this study, it was observed that the morphological structures of the foams were irregular. This situation was related to bleached kraft pulp fibers which were in macro size and these macro-dimensional fibers disrupted the cell structures and spaces. On the other hand, some studies showed that foams produced from natural polymers derivatives such as deoxyribonucleic acid sodium salt, chitosan⁷⁵, hemicellulose citrate⁸⁴, silica⁷² had irregular and open-cell pore structures. That results were similar to our study.

3.5. Antibacterial activity test

The antibacterial properties of PVAc foams reinforced with bleached kraft pulp, zinc borate and water-soluble chitosan were researched against gram-negative *Escherichia coli* and gram-positive *Staphylococcus aureus* bacteria. PVAc

foams were measured inhibition zones around disks against *Escherichia coli* and *Staphylococcus aureus* (Table 3).

When Table 3 was examined, it was determined that the Z-coded samples did not show antibacterial properties. Although all samples have no antibacterial effect against *E. coli* bacteria (Figure 7a), all C coded samples which excepted C-4 and C-7 showed antibacterial effect against *S. aureus* bacteria (Figure 7b).

It was determined that as the molecular weight of water-soluble chitosan decreased, its effectiveness increased on *S. aureus* bacteria. Also, the antibacterial effect of foams directly proportionates to the amount of water-soluble chitosan. The reason why the samples were not effective against *E. coli* bacteria in this study; It was thought that the chitosan concentration lower than previous studies^{85,86}. On the other hand, it has been reported earlier gram-negative bacteria are more resistant to antibacterial polymers and even show no effect, compared to gram-positive bacteria^{87,88}. Gram-positive bacteria have a mesh-like peptidoglycan coating that allows polymers to penetrate more easily⁸⁹. In previous studies, foams which produced from cellulose and antibacterial thermoplastic starch proved to the effectiveness against *E. coli*²⁷. Polyvinylamine and chitosan were added during

Table 3. Diameters of inhibition zones against *E. coli* and *S. aureus*.

Codes	Inhibition Zones Diameter (mm)	
	<i>E. coli</i>	<i>S. aureus</i>
Streptomycin 30 µg (Control)	13 (1.60) A	14 (2.60) A, B
Z-1	0 (-) B	0 (-) D
Z-2	0 (-) B	0 (-) D
Z-3	0 (-) B	0 (-) D
C-1	0 (-) B	13 (6.60) A
C-2	0 (-) B	15 (6.20) B, C
C-3	0 (-) B	16 (7.60) C
C-4	0 (-) B	0 (-) D
C-5	0 (-) B	13 (5.20) A
C-6	0 (-) B	16 (4.30) C
C-7	0 (-) B	0 (-) D
C-8	0 (-) B	14 (8.60) A, B
C-9	0 (-) B	14 (5.80) A, B

Note: Parentheses indicate the coefficient of variation (CV, %). A, B, C, and D letters indicate the significant differences between the groups.

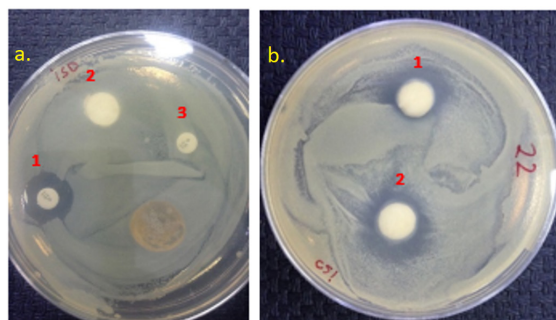


Figure 7. a. Antimicrobial activity of foams against *E. coli* (1. Control, 2. C-5, 3. C-6), b. Antimicrobial activity of foams against *S. aureus* (1. C-5, 2. C-6).

the foam production to give the foams water-stability and antibacterial properties. Manufactured foams detected to have a good resistant to *Aspergillus brasiliensis*, a sporulating mold and *Escherichia coli*, a common model bacteria³⁴. Another study stated that hydrophobically modified chitosan foams had water resistant and very effective for removing bacteria from solution as demonstrated by *Escherichia coli* and *Staphylococcus aureus* bacteria. However, produced foams showed a much better bacteria removal performance to *Escherichia coli*⁹⁰.

There are various approaches to the mechanism of action of chitosan on bacteria. First approach, electrostatic interaction occurs between the negatively charged bacteria cell walls and the positively charged chitosan, changing the permeability properties of the cell wall membrane. As a result, imbalances occur in osmotic pressure and inhibit the growth of cells. In addition, when chitosan leaks into the cell, it forms complex structures with lipids, fats and proteins. Thus, the cell cannot benefit from lipid, fat and protein. Since this mechanism is based on electrostatic interaction, it is thought that the antimicrobial effect will increase as the number of cationized amines increases⁸⁵. Another approach is thought to be due to the fact that chitosan binds to bacterial DNA and prevents mRNA formation⁹¹.

Studies with quaternary salts of chitosan were shown that antimicrobial activity against bacteria was greater than chitosan⁹². It was stated that the activity of unmodified chitosan against *E. coli* was 20 fold lower than chitosan modified with N-propyl-N,N-dimethyl, which means that derivatives with cationic charge had especially high activity against bacteria⁹³. At neutral pH, the degree of protonation of NH_2 was very low, so the repulsion of NH_3^+ was weak. Under these conditions, intramolecular and intermolecular hydrogen bonds result in the formation of micro-domains that form hydrophobic and hydrophilic parts in the polymer chain. These results related to the interaction between the bacterial cell wall and water-soluble chitosan^{85,94}.

3.6. Accelerated weathering test and color measurement

Accelerated weathering test is the most commonly used method for estimating the resistance in the characteristics

of the tested material over time. This is a simulated version of natural weathering test in a shorter time frame⁹⁵. When foams are exposed to accelerated weathering and their some properties deteriorate. It gives information about application field where foams can be used. Before and after 50 hours accelerated weathering, foams can be seen in Figure 8.

The accelerated weathering test was terminated in a short time like 50 hours. Due to the heat, UV light and sprayed water were deteriorated the structure of PVAc which used as the matrix. When PVAc subject to UV light, heat and moisture, the photochemical deacetylation reactions occur such as oxygen derivatives and alkenes chains⁹⁶. Therefore, PVAc foams have a short service life at outdoor applications.

As a result of the accelerated aging test, materials exposed to color change. L^* , a^* , b^* values of PVAc foams before and after accelerated weathering and the changes of ΔE of PVAc foams after 50 hours accelerated weathering were given in Table 4.

When the color values are examined before accelerated weathering in Table 4, L^* , a^* , b^* values of the PVAc foams were ranged from 86.52 to 92.20, -0.30 to -0.80, and 0.76 to 9.44, respectively. It was determined that the a^* value and b^* values of the samples increased after accelerated weathering. According to the color difference results of the samples, C-2 gave the highest value. The main reason for this change was that the chitosan solution had a yellowish color. As a result, b^* values of the foams were increased. As seen in Figure 9, the lowest total color difference of the samples gave Z-3.

In Figure 9, the difference in total color changes were very insignificant with increasing zinc borate. This result can be explained by the instability of zinc borate under the weathering conditions. Zinc borate was leached or hydrolysed by water or oxidized by UV light⁹⁷. On the other hand, total color changes of addition of water-soluble chitosan were higher than zinc borate. PVAc foams which included water soluble chitosan led to yellowing. This situation was attributed to the formation of carbonyl groups and the cleavage of glycosidic bonds during thermooxidation and photooxidation⁹⁸. Due to the carbonyl functional groups released from the chromophore groups⁹⁹, the total color change of the water-soluble chitosan added samples increased. In the other study, foams produced

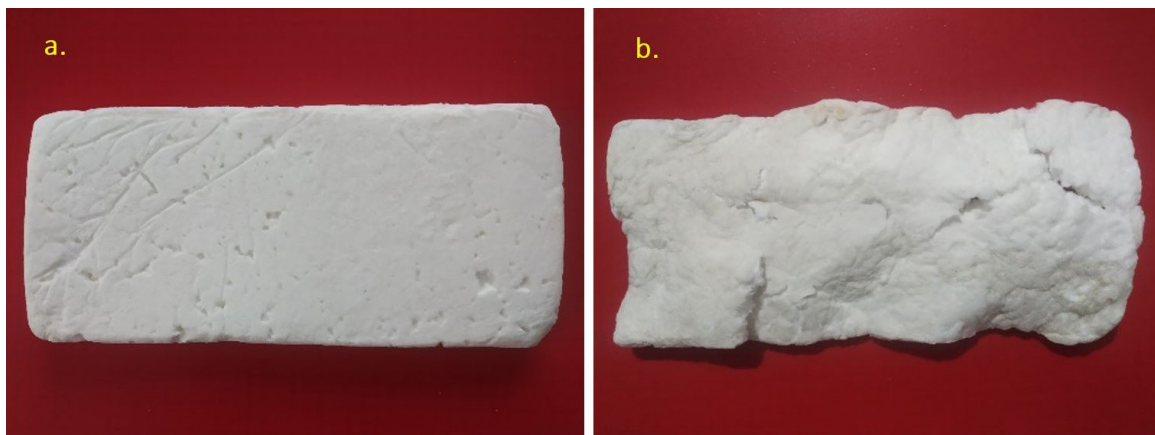
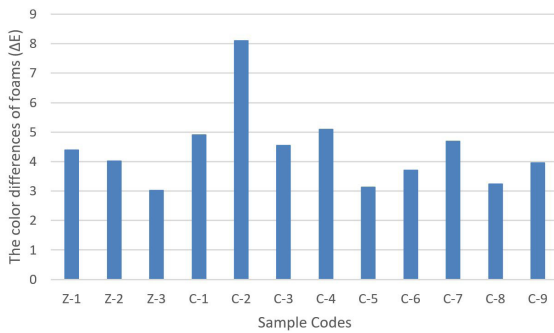


Figure 8. PVAc foams before (a), after (b) the accelerated weathering test.

Table 4. Total color changes of foams.

Codes	Before accelerated weathering			After accelerated weathering			After accelerated weathering
	L	a	b	L	a	b	ΔE
Z-1	94.44	-0.40	3.68	91.36	1.10	7.40	4.39 (8.40) A
Z-2	93.84	-0.42	4.00	91.10	-0.04	8.16	4.02 (9.00) A
Z-3	93.84	-0.50	3.30	92.20	-0.30	6.44	3.02 (8.70) B
C-1	88.28	-0.40	0.76	86.68	-0.30	11.40	4.90 (3.69) C
C-2	92.68	-0.80	3.70	85.90	0.02	13.12	8.09 (1.81) D
C-3	86.52	-0.30	8.56	83.20	-0.80	13.20	4.54 (4.68) A, C
C-4	90.20	-0.40	6.70	86.28	-0.30	11.84	5.09 (10.37) C
C-5	86.52	-0.40	8.44	85.90	0	13.02	3.12 (5.12) B
C-6	87.30	-0.30	9.44	84.84	-0.60	13.10	3.71 (11.87) F
C-7	90.20	-0.40	6.70	86.68	-0.30	11.44	4.69 (8.70) A
C-8	86.84	-0.40	8.52	85.90	0	13.08	3.24 (9.51) B, G
C-9	87.60	-0.30	9.44	84.84	-0.60	13.38	3.95 (5.96) A, F

Note: Parentheses indicate the coefficient of variation (CV, %). A, B, C, D, E, F, and G letters indicate the significant differences between the groups.

**Figure 9.** Total color differences of bio polymers reinforced foams.

from sugar cane fiber, chitosan, starch, and polyvinyl alcohol were increased amount of chitosan, the b^* color parameter increased¹⁰⁰.

4. Conclusions

This study focuses on optimized freeze-drying production process for obtaining highly porous foams and investigation of their physical and morphological properties. The process enables the fabrication of foams with high porosity, up to 87.50% and a low density of 0.12 g/cm³. The optimal reinforcements concentration is found as the compromise between two competing requirements: (i) a concentration as low as possible, to reduce zinc borate and water-soluble chitosan mass and increase porosity; and (ii) a high-water soluble chitosan concentration to avoid foam collapse upon drying. As a result of the accelerated weathering tests, PVAc foam showed low resistance to be used for outdoor application. The color differences of foam which included water-soluble chitosan were so distinctive at end of 50 hours. The foams containing water soluble chitosan had inhibitory activity against *S. aureus*. It was determined that water-soluble chitosan had more effective antimicrobial activity when both the molecular weight of chitosan was decreased, and the amount of chitosan was increased. On the other hand,

more deeply study of some toxicity test will be performed in upcoming study.

These features highlight the high potential of multifunctionality of PVAc foams as porous materials including packaging materials, medical boxes. Other potential indoor and outdoor applications can be provided with hydrophobicity modification of the foams.

5. Acknowledgments

This work was financially supported by Scientific Research Project at Mugla Sıtkı Kocman University (Project No: 17/246 and 18/012). Authors have a patent pending for this study (TURK PATENT, Application number: 2021/013967). The authors would like to express their sincere thanks to Prof. Dr. Nurettin ŞAHİN who determined the antibacterial activity of the foams from Faculty of Education in Mugla Sıtkı Kocman University.

6. References

- Jin F-L, Zhao M, Park M, Park S-J. Recent trends of foaming in polymer processing: a review. *Polymers*. 2019;11(6):953.
- Wang Y, Li J, Lv D, Jiang N, Zhang Y. Analysis of the dangerous consequences of storing pentane in polyurethane foam enterprises. In: Huang C, Nivolianitou Z, editors. Risk analysis based on data and crisis response beyond knowledge. London: CRC Press; 2019.
- Bledzki AK, Faruk O. Injection moulded microcellular wood fibre–polypropylene composites. *Compos, Part A Appl Sci Manuf*. 2006;37(9):1358-67.
- Park CB, Cheung LK. A study of cell nucleation in the extrusion of polypropylene foams. *Polym Eng Sci*. 1997;37(1):1-10.
- Zhang X, Teng Z, Huang R, Catchmark J. Biodegradable starch/chitosan foam via microwave assisted preparation: morphology and performance properties. *Polymers*. 2020;12(11):2612.
- Yildirim N, Erdonmez FS, Ozen E, Avci E, Yeniocak M, Acar M, et al. Fire-retardant bioproducts for green buildings. In: Pacheco-Torgal F, Ivanov V, Tsang DCW, editors. Bio-based materials and biotechnologies for eco-efficient construction. Cham: Woodhead Publishing; 2020. p. 67-79. (Woodhead Publishing Series in Civil and Structural Engineering).

7. Trejo AG. Fungal degradation of polyvinyl acetate. *Ecotoxicol Environ Saf.* 1988;16(1):25-35.
8. Amann M, Minge O. Biodegradability of Poly(vinyl acetate) and Related Polymers. In: Rieger B, Künkel A, Coates GW, Reichardt R, Dinjus E, Zevaco TA, editors. *Synthetic biodegradable polymers*. Berlin: Springer; 2012. p. 137-172. (Advances in Polymer Science).
9. Liu L, Guo H, Zeng X, Lai X. Preparation and properties of PVAc-nano-OMMT/PP-EVA composite. *Acta Materiae Compositae Sinica.* 2011;28(2):64-9.
10. Dubininkas M. Production and characterization of 3-methacryloxypropyltrimethoxysilane modified polyvinyl acetate dispersion. *J Chem Chem Eng.* 2016;65(3-4):119-26.
11. Ergün ME, Özen E, Yildirim N, Dalkılıç B. Manufacture of wood fiber reinforced polyvinyl acetate rigid foams. *Ormancılık Araştırma Dergisi.* 2020;7(2):104-12.
12. Cakır R, Öksüz M. Polivinilasetat (pvc) emülsiyon kompozitlerinin mekanik ve morfolojik özellikleri. *Gazi Üniv Müh Mim Fak Der.* 2013;27(3):481-90.
13. Pracella M, Haque MM, Alvarez DPV. Preparation and characterization of PLA nanocomposites with nanocellulose filled PVAC. In: *European Conference on Composite Materials*; 2012; Venice, Italy. Proceedings. Padova: University of Padova; 2012. p. 24-8.
14. Garcia de Rodriguez NL, Thielemans W, Dufresne A. Sisal cellulose whiskers reinforced polyvinyl acetate nanocomposites. *Cellulose.* 2006;13(3):261-70.
15. Hu X, Sun J, Li X, Qian L, Li J. Effect of phosphorus-nitrogen compound on flame retardancy and mechanical properties of polylactic acid. *J Appl Polym Sci.* 2021;138(7):49829.
16. Nagamine S, Mizuno Y, Hikima Y, Okada K, Wang L, Ohshima M. Reinforcement of polypropylene by cellulose microfibrils modified with polydopamine and octadecylamine. *J Appl Polym Sci.* 2021;138(7):49851.
17. Al-Saleh MH, Sundararaj U. Review of the mechanical properties of carbon nanofiber/polymer composites. *Compos, Part A Appl Sci Manuf.* 2011;42(12):2126-42.
18. Coleman JN, Khan U, Blau WJ, Gun'ko YK. Small but strong: a review of the mechanical properties of carbon nanotube-polymer composites. *Carbon.* 2006;44(9):1624-52.
19. Ozen E, Yildirim N, Dalkilic B, Ergun ME. Effects of microcrystalline cellulose on some performance properties of chitosan aerogels. *Maderas Cienc Tecnol.* 2021;(23):1-10.
20. Bülbül Ş, Akçakale N, Yaşar M, Gökmeşe H. The effect of wood ash on the mechanical properties of rubber compounds. *Mater Tehnol.* 2019;53(3):333-9.
21. Bulbul S, Yasar M, Akcakale N. Effect of changing of filling materials in NR-SBR type elastomer based rubber materials on mechanical properties. *Polymer.* 2014;38(5):664-70.
22. Yi T, Zhao H, Mo Q, Pan D, Liu Y, Huang L, et al. From cellulose to cellulose nanofibrils: a comprehensive review of the preparation and modification of cellulose nanofibrils. *Materials.* 2020;13(22):5062.
23. Komal UK, Lila MK, Singh I. Processing of PLA/pineapple fiber based next generation composites. *Mater Manuf Process.* 2021. In press.
24. Pickering K. *Properties and performance of natural-fibre composites*. Cambridge: Elsevier; 2008.
25. Peelman N, Ragaert P, De Meulenaer B, Adons D, Peeters R, Cardon L, et al. Application of bioplastics for food packaging. *Trends Food Sci Technol.* 2013;32(2):128-41.
26. Petersen K, Væggemose Nielsen P, Bertelsen G, Lawther M, Olsen MB, Nilsson NH, et al. Potential of biobased materials for food packaging. *Trends Food Sci Technol.* 1999;10(2):52-68.
27. Heydarifard S, Pan Y, Xiao H, M. Nazhad M, Shipin O. Water-resistant cellulosic filter containing non-leaching antimicrobial starch for water purification and disinfection. *Carbohydr Polym.* 2017;163:146-52.
28. Ashjari HR, Dorraji MSS, Fakhrzadeh V, Eslami H, Rasoulifard MH, Rastgouy-Houjaghan M, et al. Starch-based polyurethane/CuO nanocomposite foam: antibacterial effects for infection control. *Int J Biol Macromol.* 2018;111:1076-82.
29. Jain S, Bhanjana G, Heydarifard S, Dilbaghi N, Nazhad MM, Kumar V, et al. Enhanced antibacterial profile of nanoparticle impregnated cellulose foam filter paper for drinking water filtration. *Carbohydr Polym.* 2018;202:219-26.
30. Jain P, Pradeep T. Potential of silver nanoparticle-coated polyurethane foam as an antibacterial water filter. *Biotechnol Bioeng.* 2005;90(1):59-63.
31. Greulich C, Kittler S, Epple M, Muhr G, Köller M. Studies on the biocompatibility and the interaction of silver nanoparticles with human mesenchymal stem cells (hMSCs). *Langenbecks Arch Surg.* 2009;394(3):495-502.
32. Kittler S, Greulich C, Diendorf J, Köller M, Epple M. Toxicity of silver nanoparticles increases during storage because of slow dissolution under release of silver ions. *Chem Mater.* 2010;22(16):4548-54.
33. Silver S. Bacterial silver resistance: molecular biology and uses and misuses of silver compounds. *FEMS Microbiol Rev.* 2003;27(2-3):341-53.
34. Ottenhall A, Seppänen T, Ek M. Water-stable cellulose fiber foam with antimicrobial properties for bio based low-density materials. *Cellulose.* 2018;25(4):2599-613.
35. Lichter JA, Rubner MF. Polyelectrolyte multilayers with intrinsic antimicrobial functionality: the importance of mobile polycations. *Langmuir.* 2009;25(13):7686-94.
36. Lichter JA, Van Vliet KJ, Rubner MF. Design of antibacterial surfaces and interfaces: polyelectrolyte multilayers as a multifunctional platform. *Macromolecules.* 2009;42(22):8573-86.
37. Vaara M. Agents that increase the permeability of the outer membrane. *Microbiol Mol Biol Rev.* 1992;56(3):395-411.
38. Rahimi SK, O'Donnell K, Haight B, Machado A, Martin C, Meng F, et al. Supercritical-CO₂ foam extrusion of hydroxypropyl methyl cellulose acetate succinate/itraconazole amorphous solid dispersions: processing-structure-property relations. *J Pharm Sci.* 2021;110(4):1444-56.
39. Hou J, Zhao G, Wang G. Polypropylene/talc foams with high weight-reduction and improved surface quality fabricated by mold-opening microcellular injection molding. *J Mater Res Technol.* 2021;12:74-86.
40. Yeh S-K, Liu Y-C, Wu W-Z, Chang K-C, Guo W-J, Wang S-F. Thermoplastic polyurethane/clay nanocomposite foam made by batch foaming. *J Cell Plast.* 2013;49(2):119-30.
41. Deng Y, Dewil R, Appels L, Ansart R, Baeyens J, Kang Q. Reviewing the thermo-chemical recycling of waste polyurethane foam. *J Environ Manage.* 2021;278:111527.
42. Chakrabarty A, Teramoto Y. Recent advances in nanocellulose composites with polymers: a guide for choosing partners and how to incorporate them. *Polymers.* 2018;10(5):517.
43. Li Y, Wang B, Sui X, Xu H, Zhang L, Zhong Y, et al. Facile synthesis of microfibrillated cellulose/organosilicon/polydopamine composite sponges with flame retardant properties. *Cellulose.* 2017;24(9):3815-23.
44. Sultana N, Wang M. PHBV/PLLA-based composite scaffolds fabricated using an emulsion freezing/freeze-drying technique for bone tissue engineering: surface modification and in vitro biological evaluation. *Biofabrication.* 2012;4(1):015003.
45. Zhang S, Zhang S, Li W, Pei Y, Liu B, Yang H. PEI-functionized cellulose foam for the visual recognition and removal of Cr(VI). *Mater Lett.* 2021;293:129685.
46. Jennings TA. *Lyophilization: introduction and basic principles*. Boca Raton: CRC Press; 2019.

47. Svagan AJ, Samir MASA, Berglund LA. Biomimetic foams of high mechanical performance based on nanostructured cell walls reinforced by native cellulose nanofibrils. *Adv Mater.* 2008;20(7):1263-9.
48. Dilamian M, Noroozi B. Rice straw agri-waste for water pollutant adsorption: relevant mesoporous super hydrophobic cellulose aerogel. *Carbohydr Polym.* 2021;251:117016.
49. Do NHN, Tran VT, Tran QBM, Le KA, Thai QB, Nguyen PTT, et al. Recycling of pineapple leaf and cotton waste fibers into heat-insulating and flexible cellulose aerogel composites. *J Polym Environ.* 2021;29(4):1112-21.
50. Lou C-W, Zhou X, Liao X, Peng H, Ren H, Li T-T, et al. Sustainable cellulose-based aerogels fabricated by directional freeze-drying as excellent sound-absorption materials. *J Mater Sci.* 2021;56(33):18762-74.
51. Yang Z, Li H, Niu G, Wang J, Zhu D. Poly(vinylalcohol)/chitosan-based high-strength, fire-retardant and smoke-suppressant composite aerogels incorporating aluminum species via freeze drying. *Compos, Part B Eng.* 2021;219:108919.
52. Hamilton V, Yuan Y, Rigney DA, Puckett AD, Ong JL, Yang Y, et al. Characterization of chitosan films and effects on fibroblast cell attachment and proliferation. *J Mater Sci Mater Med.* 2006;17(12):1373-81.
53. Kasaai MR, Arul J, Charlet G. Intrinsic viscosity-molecular weight relationship for chitosan. *J Polym Sci, B, Polym Phys.* 2000;38(19):2591-8.
54. Dutta PK, Dutta J, Tripathi VS. Chitin and chitosan: chemistry, properties and applications. *J Sci Ind Res.* 2004;63(1):20-31.
55. Li R, Guo Z, Jiang P. Synthesis, characterization, and antifungal activity of novel quaternary chitosan derivatives. *Carbohydr Res.* 2010;345(13):1896-900.
56. Dufresne A. Nanocellulose: from nature to high performance tailored materials. Berlin: Walter de Gruyter GmbH & Co KG; 2017.
57. Savastano H Jr, Fiorelli J, Santos SFD. Sustainable and nonconventional construction materials using inorganic bonded fiber composites. Cambridge: Woodhead Publishing; 2017.
58. Fan M, Fu F. Advanced high strength natural fibre composites in construction. London: Woodhead Publishing; 2016.
59. Kandemir A, Pozegic TR, Hamerton I, Eichhorn SJ, Longana ML. Characterisation of natural fibres for sustainable discontinuous fibre composite materials. *Materials.* 2020;13(9):2129.
60. Monteiro SN, Lopes FPD, Barbosa AP, Bevitore AB, Silva ILAD, Costa LLD. Natural lignocellulosic fibers as engineering materials: an overview. *Metall Mater Trans, A Phys Metall Mater Sci.* 2011;42(10):2963.
61. Martoia F, Cochereau T, Dumont PJJ, Orgéas L, Terrien M, Belgacem MN. Cellulose nanofibril foams: links between ice-templating conditions, microstructures and mechanical properties. *Mater Des.* 2016;104:376-91.
62. Hossen MR, Talbot MW, Kennard R, Bousfield DW, Mason MD. A comparative study of methods for porosity determination of cellulose based porous materials. *Cellulose.* 2020;27(12):6849-60.
63. Wainwright SA, Gosline JM, Biggs WD, Currey JD. Mechanical design in organisms. Princeton: Princeton University Press; 1982.
64. Sehaqui H, Zhou Q, Berglund LA. High-porosity aerogels of high specific surface area prepared from nanofibrillated cellulose (NFC). *Compos Sci Technol.* 2011;71(13):1593-9.
65. Pääkkö M, Vapaavuori J, Silvennoinen R, Kosonen H, Ankerfors M, Lindström T, et al. Long and entangled native cellulose I nanofibers allow flexible aerogels and hierarchically porous templates for functionalities. *Soft Matter.* 2008;4(12):2492-9.
66. Aulin C, Netrval J, Wågberg L, Lindström T. Aerogels from nanofibrillated cellulose with tunable oleophobicity. *Soft Matter.* 2010;6(14):3298-305.
67. Cervin NT, Aulin C, Larsson PT, Wågberg L. Ultra porous nanocellulose aerogels as separation medium for mixtures of oil/water liquids. *Cellulose.* 2012;19(2):401-10.
68. Sehaqui H, Zhou Q, Ikkala O, Berglund LA. Strong and tough cellulose nanopaper with high specific surface area and porosity. *Biomacromolecules.* 2011;12(10):3638-44.
69. Liu Y, Lu P, Xiao H, Heydarifard S, Wang S. Novel aqueous spongy foams made of three-dimensionally dispersed wood-fiber: entrapment and stabilization with NFC/MFC within capillary foams. *Cellulose.* 2017;24(1):241-51.
70. Tillotson TM, Hrubesh LW. Transparent ultralow-density silica aerogels prepared by a two-step sol-gel process. *J Non-Cryst Solids.* 1992;145:44-50.
71. Cervin NT, Andersson L, Ng JBS, Olin P, Bergström L, Wågberg L. Lightweight and strong cellulose materials made from aqueous foams stabilized by nanofibrillated cellulose. *Biomacromolecules.* 2013;14(2):503-11.
72. Wang J, Zhou Q, Song D, Qi B, Zhang Y, Shao Y, et al. Chitosan-silica composite aerogels: preparation, characterization and Congo red adsorption. *J Sol-Gel Sci Technol.* 2015;76(3):501-9.
73. Vasconcelos NF, Andrade FK, Vieira LAP, Vieira RS, Vaz JM, Chevallier P, et al. Oxidized bacterial cellulose membrane as support for enzyme immobilization: properties and morphological features. *Cellulose.* 2020;27(6):3055-83.
74. Kaisangri N, Kerdechueen O, Laohakunjit N. Biodegradable foam tray from cassava starch blended with natural fiber and chitosan. *Ind Crops Prod.* 2012;37(1):542-6.
75. Pakompadungsit P, Prasopdee T, Swainson NM, Chworos A, Smitthipong W. DNA:chitosan complex, known as a drug delivery system, can create a porous scaffold. *Polym Test.* 2020;83:106333.
76. Pojanavaraphan T, Magaraphan R, Chiou B-S, Schiraldi DA. Development of biodegradable foamlike materials based on casein and sodium montmorillonite clay. *Biomacromolecules.* 2010;11(10):2640-6.
77. Ferreira ES, Rezende CA, Cranston ED. Fundamentals of cellulose lightweight materials: bio-based assemblies with tailored properties. *Green Chem.* 2021;23(10):3542-68.
78. Wang L, Sánchez-Soto M, Abt T, MasPOCH ML, Santana OO. Microwave-crosslinked bio-based starch/clay aerogels. *Polym Int.* 2016;65(8):899-904.
79. MacKenzie RC. Clay - water relationships. *Nature.* 1953;171(4355):681-3.
80. Bakeeva IV, Doktorova AV, Damshkaln LG, Lozinsky VI. A study of cryostructuring of polymer systems. 54. Hybrid organo-inorganic poly(vinyl alcohol) cryogels filled with in situ formed silica. *Colloid J.* 2021;83(1):49-63.
81. Dash R, Li Y, Ragauskas AJ. Cellulose nanowhisker foams by freeze casting. *Carbohydr Polym.* 2012;88(2):789-92.
82. Svagan AJ, Azizi Samir MAS, Berglund LA. Biomimetic polysaccharide nanocomposites of high cellulose content and high toughness. *Biomacromolecules.* 2007;8(8):2556-63.
83. Li R, Du J, Zheng Y, Wen Y, Zhang X, Yang W, et al. Ultralightweight cellulose foam material: preparation and properties. *Cellulose.* 2017;24(3):1417-26.
84. Salam A, Venditti RA, Pawlak JJ, El-Tahlawy K. Crosslinked hemicellulose citrate-chitosan aerogel foams. *Carbohydr Polym.* 2011;84(4):1221-9.
85. Goy RC, Britto D, Assis OBG. A review of the antimicrobial activity of chitosan. *Polimeros.* 2009;19(3):241-7.
86. Netanel Liberman G, Ochbaum G, Bitton R. (Malis) Arad S. Antimicrobial hydrogels composed of chitosan and sulfated polysaccharides of red microalgae. *Polymer.* 2021;215:123353.
87. Özderin S. Determination of some chemical properties of wild pear (*Pyrus spinosa* Forsk.). *BioResources.* 2022;17(1):1659-69.
88. Biswas B, Rogers K, McLaughlin F, Daniels D, Yadav A. Antimicrobial activities of leaf extracts of guava (*Psidium guajava* L.) on two gram-negative and gram-positive bacteria. *Int J Microbiol.* 2013;2013:e746165.

89. Rameshkumar KB, George V, Shiburaj S. Chemical constituents and antibacterial activity of the leaf oil of *Cinnamomum chemungianum* Mohan et Henry. *J Essent Oil Res.* 2007;19(1):98-100.
90. Vo D-T, Lee C-K. Antimicrobial sponge prepared by hydrophobically modified chitosan for bacteria removal. *Carbohydr Polym.* 2018;187:1-7.
91. Eikenes M, Alfredsen G, Christensen BE, Militz H, Solheim H. Comparison of chitosans with different molecular weights as possible wood preservatives. *J Wood Sci.* 2005;51(4):387-94.
92. Sadeghi AMM, Amini M, Avadi MR, Siedi F, Rafiee-Tehrani M, Junginger HE. Synthesis, characterization, and antibacterial effects of trimethylated and triethylated 6-NH₂-6-deoxy chitosan. *J Bioact Compat Polym.* 2008;23(3):262-75.
93. Muxika A, Etxabide A, Uranga J, Guerrero P, de la Caba K. Chitosan as a bioactive polymer: processing, properties and applications. *Int J Biol Macromol.* 2017;105:1358-68.
94. Xie W, Xu P, Wang W, Liu Q. Preparation and antibacterial activity of a water-soluble chitosan derivative. *Carbohydr Polym.* 2002;50(1):35-40.
95. Liszkowska J, Moraczewski K, Borowicz M, Paciorek-Sadowska J, Czupryński B, Isbrandt M. The effect of accelerated aging conditions on the properties of rigid polyurethane-polyisocyanurate foams modified by cinnamon extract. *Appl Sci.* 2019;9(13):2663.
96. Bubev E, Georgiev A, Machkova M. ATR-FTIR spectroscopy study of the photodegradation protective properties of BP-4 and 4HBP in polyvinyl acetate thin films. *J Mol Struct.* 2016;1118:184-93.
97. Bussiere P-O, Gardette J-L, Rapp G, Masson C, Therias S. New insights into the mechanism of photodegradation of chitosan. *Carbohydr Polym.* 2021;259:117715.
98. Lizárraga-Laborín LL, Quiroz-Castillo JM, Encinas-Encinas JC, Castillo-Ortega MM, Burruel-Ibarra SE, Romero-García J, et al. Accelerated weathering study of extruded polyethylene/poly (lactic acid)/chitosan films. *Polym Degrad Stabil.* 2018;155:43-51.
99. Turku I, Kärki T. Accelerated weathering of fire-retarded wood-polypropylene composites. *Compos, Part A Appl Sci Manuf.* 2016;81:305-12.
100. Debiagi F, Mali S, Grossmann MVE, Yamashita F. Biodegradable foams based on starch, polyvinyl alcohol, chitosan and sugarcane fibers obtained by extrusion. *Braz Arch Biol Technol.* 2011;54(5):1043-52.